GEOPHYSICAL RESEARCH LETTERS, VOL. 39, L04704, doi:10.1029/2011GL050610, 2012

Long tails in regional surface temperature probability distributions with implications for extremes under global warming

Tyler W. Ruff[1,2] and J. David Neelin[1,3]

Received 9 December 2011; revised 24 January 2012; accepted 24 January 2012; published 25 February 2012.

[1] Prior work has shown that probability distributions of column water vapor and several passive tropospheric chemical tracers exhibit longer-than-Gaussian (approximately exponential) tails. The tracer-advection prototypes explaining the formation of these long-tailed distributions motivate exploration of observed surface temperature distributions for non-Gaussian tails. Stations with long records in various climate regimes in National Climatic Data Center Global Surface Summary of Day observations are used to examine tail characteristics for daily average, maximum and minimum surface temperature probability distributions. Each is examined for departures from a Gaussian fit to the core (here approximated as the portion of the distribution exceeding 30% of the maximum). While the core conforms to Gaussian for most distributions, roughly half the cases exhibit non-Gaussian tails in both winter and summer seasons. Most of these are asymmetric, with a long, roughly exponential, tail on only one side. The shape of the tail has substantial implications for potential changes in extreme event occurrences under global warming. Here the change in the probability of exceeding a given threshold temperature is quantified in the simplest case of a shift in the present-day observed distribution. Surface temperature distributions with long tails have a much smaller change in threshold exceedances (smaller increases for high-side and smaller decreases for low-side exceedances relative to exceedances in current climate) under a given warming than do near-Gaussian distributions. This implies that models used to estimate changes in extreme event occurrences due to global warming should be verified regionally for accuracy of simulations of probability distribution tails. **Citation:** Ruff, T. W., and J. D. Neelin (2012), Long tails in regional surface temperature probability distributions with implications for extremes under global warming, *Geophys. Res. Lett.*, *39*, L04704, doi:10.1029/2011GL050610.

1. Introduction

[2] Understanding the nature of potential changes in the probability of extreme climate/weather events in the context of global warming is vital for future risk management and assessment of agricultural, economic and ecosystem consequences [*Meehl et al.*, 2000; *Parmesan et al.*, 2000; *Christensen et al.*, 2007; *Schlenker and Roberts*, 2009]. There are indications that high extreme temperature anomalies have become more frequent and larger in magnitude in many regions during the past century, and that the occurrence and magnitude of cold extreme anomalies have weakened [*Alexander et al.*, 2006; *Caesar et al.*, 2006] although there can be considerable differences among regions or temperature variables such as daily maximum and minimum or extreme cold outbreaks [*Easterling et al.*, 2000; *Walsh et al.*, 2001]. Both global and regional scale climate models project changes in the occurrences of temperature extremes under global warming [e.g., *Meehl et al.*, 2007; *Kharin et al.*, 2007; *Christensen et al.*, 2007; *Diffenbaugh et al.*, 2007].

[3] As a baseline for a model validation and to gain insight into the natural variability processes responsible for extreme temperature events, it is useful to examine properties of the tails of the probability distributions in station observations of air temperature. In doing so, there is reason to believe that fine-scale processes will be important [*Diffenbaugh et al.*, 2005], suggesting a comparison on local to regional scales. Furthermore, recent observational and theoretical results for transport processes suggest the likelihood of distinct tail properties. Non-Gaussian tails (most of which are approximately exponential) occur very commonly in probability distributions of passive tropospheric chemical tracers and water vapor [*Neelin et al.*, 2010], and their existence is consistent with simple mathematical prototypes for passive tracer advection problems with a forcing that maintains a gradient [e.g., *Bourlioux and Majda*, 2002; *Pierrehumbert*, 2000; *Ngan and Pierrehumbert*, 2000; *Majda and Gershgorin*, 2010]. Such long-tailed distributions are hypothesized to occur in near-surface air temperature data since a large portion of near-surface air temperature variability is associated with advection of air masses across a large-scale temperature gradient. Although air temperature is not a passive tracer and potentially has complications due to effects of soil moisture [*Diffenbaugh et al.*, 2007] and clouds, there is still ample reason to expect that probability density functions (PDFs) of temperature might commonly inherit key properties seen in both the observed tracer distributions and the prototypes. Specifically, the tails of the PDF can be longer (often approximately exponential) than would be anticipated from a fit to the core of the PDF (i.e., a central region containing the bulk of the distribution, often approximately Gaussian). We can further anticipate asymmetry in these tails since asymmetry was noted in certain of the observed tracers, and can be easily produced in the prototypes, for instance, if the gradient on the high-tracer side of the region of interest differs from the gradient on the low-tracer side or if the advecting flow has an asymmetry between shorter intense flow events in one direction versus longer, less intense flow events in the other [*Neelin et al.*, 2010]. Other effects can also contribute to long tails in geophysical

[1]Department of Atmospheric and Oceanic Sciences, University of California, Los Angeles, California, USA.
[2]Commodity Weather Group, Bethesda, Maryland, USA.
[3]Institute of Geophysics and Planetary Physics, University of California, Los Angeles, California, USA.

0094-8276/12/2011GL050610

applications related to temperature, including multiplicative noise processes such as a stochastic damping [*Sura and Sardeshmukh*, 2008; *Sura and Perron*, 2010].

[4] The influence of tail behavior on the risk of extreme events under global warming underlies the pragmatic importance of quantifying tail characteristics. The commonly stated qualitative explanation [e.g., *Meehl et al.*, 2000, 2007; *Trenberth et al.*, 2007; *Walker and Diffenbaugh*, 2008] for changes in extreme events under global warming is of a shift in the mean causing an increase in the frequency of events exceeding a certain threshold value, or conversely a decrease in the occurrences of temperatures below a certain threshold (such as freezing temperature or chill temperature relevant to certain agricultural products). While this overall picture remains, the presence of non-Gaussian tails implies that a change in such distributions can potentially have more complex behavior than that of a pure Gaussian, which can be characterized simply by the mean and standard deviation. A dependence on gradient and flow characteristics in the region of interest is one possible complication suggested by the simple prototypes, so locations in various climate regimes are examined in Section 3. Once the existence of long-tailed behavior is established, as is the aim here, the behavior of the distribution under global warming becomes potentially more complex; relatively simple changes, for instance in zonal wind, potentially alter the properties of such tails [*Majda and Gershgorin*, 2012]. Here we show that even in the simplest case where climate change is assumed to shift the distribution with increasing temperature, the form of the tails has a dramatic impact on the increase of the probability of exceeding a given threshold temperature, as discussed in Section 4.

2. Data and Methods

[5] The data product used in this paper is the Global Surface Summary of Day (GSOD) version 7, produced by the National Climatic Data Center (NCDC), consisting of 18 daily surface meteorological variables. The input data are derived from the synoptic/hourly observations contained in U.S. Air Force DATSAV3 Surface data and Federal Climate Complex Integrated Surface Data (ISD) [*Lott et al.*, 2008]. Most stations discussed in this paper are from within the United States owing to the relatively long length of the time series, typically spanning from around 1950 through 2009. Effort was made to only include stations with relatively few missing values and no other major data quality issues. Comparison of the GSOD data to the corresponding NCDC Global Historical Climatology Network (GHCN) version 1 daily station data [*Peterson and Vose*, 1997] at several stations showed no significant differences.

[6] The three temperature variables of focus are the daily maximum ($T_{\max}$), daily average (T_{avg}), and daily minimum ($T_{\min}$), and the corresponding distributions are shown for each station over JJA (June, July, August) or DJF (December, January, February). To remove potential biases owing to multi-decadal warming or cooling, the time series are linearly detrended. The seasonal cycle is removed by subtracting the daily climatology, calculated as the mean of each calendar day over all years in the time domain (leap days were removed for simplicity), which proved sufficiently smooth due to the long time series considered here.

[7] The probability distributions are plotted as histograms using a bin width of 5/9°C (except where noted otherwise) to prevent artifacts from the conversion from Fahrenheit to Celsius. A Gaussian curve is shown on each distribution for reference. One could define the curve with the standard deviation σ of the entire distribution, but this would be affected by the presence of non-Gaussian tails. Therefore, the Gaussian is fit to the core of the distribution by polynomial regression, which we chose to be all points exceeding a threshold of 0.3 of the distribution maximum. At this threshold, the σ of the core is typically only ~5–15% less than the value of σ for the entire distribution (with the exception of stations with the most marked tails, e.g., LAX Airport, Los Angeles, CA, Long Beach, CA, and San Juan, Puerto Rico). Lower thresholds decrease this value by a few percent but the fit becomes overly skewed by tails, while higher thresholds rapidly increase the σ difference and tends to inflate the appearance of tails. A few instances were found with departures from Gaussian so marked that even the cores exhibit differences from a Gaussian fit.

[8] To assess statistical significance of the tails, an error envelope is created by sampling artificial time series from a Gaussian first-order autoregressive [AR(1)] process that approximates the core. The AR(1) process is chosen to match the standard deviation and 1-day autocorrelation time for each station and season. The process fits the observed autocorrelation at lags to at least several days to a week. For each distribution, the error statistic is calculated by simulating 1000 artificial time series the same length as the station data and computing each of the 1000 histograms as was done for the observations. A confidence interval is constructed using the 5th to 95th percentiles of the spread in each bin. That is, the top of the confidence interval exceeds 95% of the values in each bin constructed from the artificial series using the same time series length and binning procedure.

3. Regional Consistencies and Differences in Probability Distributions

[9] Figure 1a displays the probability distributions of daily temperature anomalies (after subtracting the climatology and detrending), with the Gaussian core fit and the AR(1) error envelope superimposed, for each of the three variables ($T_{\max}$, T_{avg}, $T_{\min}$) during JJA (summer) at the four stations LAX Airport, Los Angeles, CA, Long Beach, CA, Phoenix, AZ, and Houston, TX. Each of the stations exhibits marked departures from Gaussian in at least two of the temperature variables in one of the tails. As expected, asymmetry is common. In each of these stations, one long tail is found, while the other either does not depart strongly from Gaussian or decreases more rapidly than the Gaussian fit to the core. This is common among stations sampled.

[10] LAX and Long Beach are chosen primarily to demonstrate the consistency among stations in similar climate configurations (coastal/Mediterranean) in close proximity (within 20 km), and both are seen to exhibit long positive tails in $T_{\max}$ and T_{avg} over the summer season. It is apparent that $T_{\max}$, T_{avg}, and $T_{\min}$ can substantially differ in tail behavior—this varies among regions. In the LAX and Long Beach cases, the positive tails in $T_{\max}$ and T_{avg} could be explained by the occasional advection of relatively hot air masses from land, while the absence of strong tails in $T_{\min}$ indicates that the minimum temperature may instead be controlled by the sea breeze and ocean air temperatures.

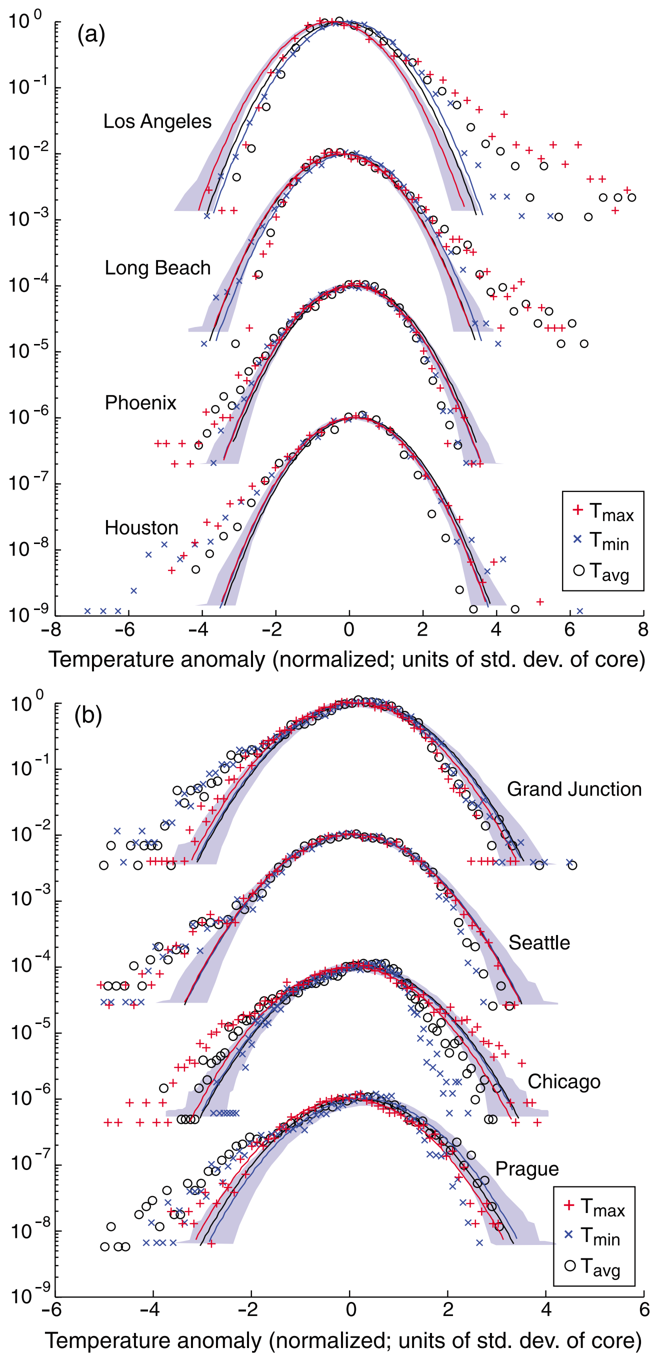

Figure 1. (a) Probability distributions (as normalized frequency of occurrence) of daily temperature anomalies, normalized by the standard deviation of a Gaussian fit to the core (fit for points exceeding 30% of the maximum, drawn as solid lines), at selected stations (vertically shifted for clarity) during JJA (summer). Stacked for each station are the variables T_{max} (red), T_{avg} (black), and T_{min} (blue). The shaded error envelope (from sampling artificial autocorrelated Gaussian time series as described in Section 2) is shown for T_{max} at each station (the envelopes for T_{avg} and T_{min} are very similar). (b) As in Figure 1a but for during DJF (winter), and the error envelope is shown for T_{min} at each station.

High-side long tails in T_{max} and T_{avg} are also present in the DJF season for these stations (not shown).

[11] The Phoenix and Houston stations, in subtropical arid and subtropical humid climate regimes, respectively, share similar distribution characteristics during JJA. Both are located in areas close to a local maximum of climatological temperature with little gradient, and thus might be anticipated to exhibit a diminished high-side tail because there is no neighboring region from which to advect a substantially warmer air mass. As discussed in detail in Section 4, the Gaussian (or shorter) nature of the positive tails in these two cities will have different implications under global warming when compared to the roughly exponential tails found in the Los Angeles stations. The Phoenix and Houston stations also exhibit cold side tails in all three variables during summer.

[12] Figure 1b displays four stations—Grand Junction, CO, Seattle, WA, Chicago, IL, and Prague, Czech Republic—in the same format as Figure 1a, except for DJF. With the exception of Seattle, these stations represent interior continental climate regimes, and all of which contain distributions with interesting tail configurations during the winter. Non-Gaussian low-side tails exist for at least two temperature variables for these stations, and asymmetry is seen in varying degrees due to the tendency for high-side tails to depart less from the Gaussian. A substantial asymmetry also exists in the cores of the Chicago and Prague stations. The tendency towards a skewed non-Gaussian core is also found in many other stations among all three variables, with the majority of such occurring in DJF and not JJA. Also interesting are the relative contributions of T_{max} and T_{min} to T_{avg}—one may expect the average temperature to fall roughly between the maximum and minimum values for a given day, as is evident in most JJA cases. However, T_{avg} seems to mimic T_{min} in the Grand Junction low-side tail, whereas T_{avg} in Prague exhibits a longer tail relative to the core than either T_{min} or T_{max}. Although we display examples of non-Gaussian low-side tails during the winter season in Figure 1b, there are also many stations that do not exhibit such long tails. The regional differences in low-side tail characteristics among stations implies that certain regions are more susceptible to changes in extreme value frequency under global warming, as mentioned for the JJA cases. In these cases, a positive shift in the mean temperature implies a decrease in the occurrences of temperatures below a certain threshold, and the tail characteristics of the distribution will help determine the probability of such a decrease. This may be of practical importance for agricultural products that are sensitive to the freezing or chill temperature.

4. Exceedance Thresholds

[13] The existence of long tails in temperature distributions–and the differing characteristics among stations–have substantial implications for changes in frequency of extreme temperature events over a particular location under gradual shift in mean temperature, as in projected global warming. Implications involving potential changes in tail properties can be addressed in simple prototypes [*Majda and Gershgorin*, 2012] or regional climate models [*Diffenbaugh et al.*, 2007]. A class of implications that can be addressed directly from the observed distributions may be inferred for

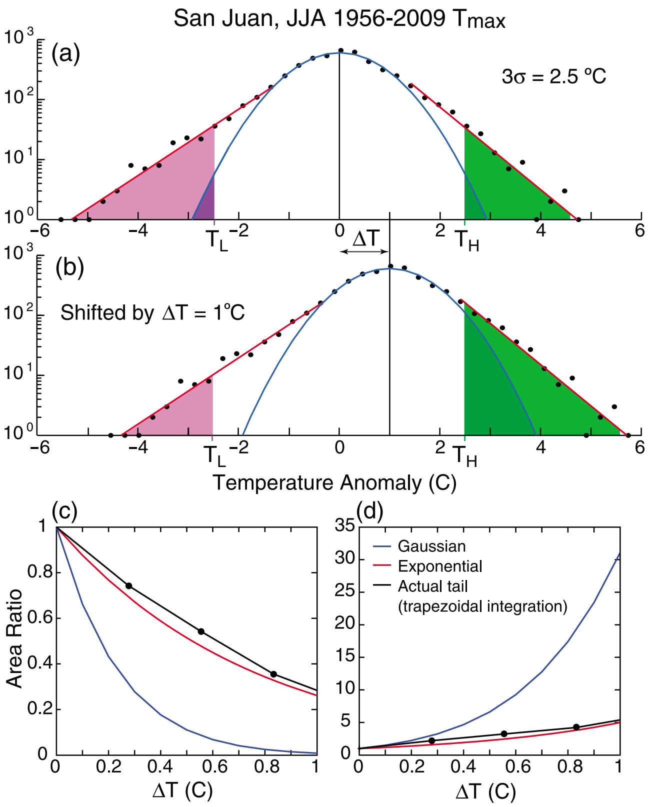

Figure 2. (a) Probability distribution function (shown as frequency of occurrence) for anomalies of daily maximum surface air temperature at San Juan, Puerto Rico (black dots). The blue curve shows a Gaussian core fit to values above 30% of maximum; the red lines show exponential fits to the low-side and high-side tails. The regions representing exceedances of a threshold value $T_H = 3\sigma = 2.5°$ C, on the high side, or $T_L = -3\sigma$ on the low side, are shown in green and purple respectively (dark shading for the corresponding region if the tails followed the Gaussian fit to the core). Exceedance probabilities are integrated between T_H or T_L and the furthest bin with nonzero values in the respective tails (note shaded regions are not area proportional on this log plot). (b) Ratio of the probability of low-side exceedance of T_L as a function of the shift ΔT of the distribution to probability in the un-shifted case, comparing this ratio for the observed tail (black), for an exponential fit to the tail (red) and for a continuation of the Gaussian corresponding to the core (using the same integration interval as for the observations). (c and d) As in Figure 2b, but for the high-side case.

the simplest case where the mean of the distribution is assumed to shift. For advection-dominated tails, this corresponds to assuming that flow statistics and temperature gradient remain constant while the large-scale background temperature increases. If tail characteristics are consequential in this simple case, they appear likely to be at least as important in more complex cases. This simple case can be discussed quantitatively by calculating the increase of the probability of exceeding a given high-side threshold temperature T_H or the decrease in low-side exceedances (i.e., falling below low-side threshold T_L) under a positive shift ΔT of the mean of the distribution. Another approach [*Kharin and Zwiers*, 2005] fits distributions of extreme occurrences in a given interval that apply asymptotically in the limit of large samples. Here we focus on assessing the potential significance of the tail properties in observed distributions, and of hence the importance of physically interpreting regional disparities. Evidence for the usefulness of a simple shift in describing observed changes is discussed, e.g., by *Simolo et al.* [2010].

[14] Figure 2 illustrates the implications of tail properties for a shift of the observed temperature anomaly distribution for San Juan, Puerto Rico, which was chosen because it has long tails on both low and high sides permitting both cases to be illustrated for a single station; it also has a clearly defined core and the tails are approximately exponential. Shaded in green in Figure 2a under the positive tail is the region of integration from the threshold temperature T_H up to the maximum nonzero bin of the distribution, representing the climatological probability of exceedance of this threshold. Here the value of T_H is chosen to be 3 standard deviations (~2.5°C for San Juan) above the mean (denoted as $T_H = 3\sigma$ hereafter). The simplest case of a positive temperature increase is illustrated by shifting the observed distribution by $\Delta T = 1$°C (~0.8σ for San Juan), with the increased probability of exceedance of T_H indicated by the green region in Figure 2b. The negative tail is integrated from the minimum nonzero bin to $T_L = -3\sigma$ and then shifted by $\Delta T = 1$°C to obtain a measure of the decrease in frequency of exceedances in this warming scenario.

[15] The magnitude of a potential increase in frequency of extreme temperature events occurring over a particular location in the future will depend on the tail characteristics of the distribution—and will differ strongly from Gaussian tails to long (e.g., approximately exponential) tails. We can quantify this difference between tail types by calculating the ratio of the probability of exceedance of T_H or T_L as a function of the shift ΔT for a given long-tailed distribution and then comparing it to the hypothetical exceedance ratio of the Gaussian fit over the same interval. Figure 2c displays exceedance ratio curves for the positive tail in San Juan for the case of the actual tail (black curve), the approximated exponential tail (red curve), and for the Gaussian fit (blue curve; note that the Gaussian fit characterizing the core is continued through the end of the observable part of the tail region when integrating). Under 1°C warming shift, this ratio for $T_H = 3\sigma$ would increase by about a factor of 30 for the Gaussian fit. However, for the actual positive tail seen in this distribution, seen closely matching the exponential fit, the probability of exceedance increases by less than a quarter of this amount for a 1°C warming and much less rapidly for larger warming. Indeed, extending to a 1.5°C warming would place the Gaussian fit at a factor of about 100 while the actual tail at only 10.

[16] Conversely, Figure 2b shows the ratio curves associated with the low-side tail integrations decreasing with increasing ΔT, representing the diminishing probability of exceeding the threshold temperature under the warming. The Gaussian ratio curve (blue curve) is seen to be diminishing much more rapidly than the actual curve (black) and the exponential fit (red curve): after a 1°C warming, there

remains a 30% exceedance probability in the actual exponential tail case, but only a 0.85% probability under the Gaussian fit.

5. Discussion and Conclusions

[17] Analysis of observational surface temperature probability distributions here finds non-Gaussian tails to be common in station measurements over a range of locations and climate zones. To provide a rough summary statistic for the 29 stations and the three temperature variables ($T_{\max}$, $T_{\min}$, and daily average) examined here, approximately half these distributions exhibit substantial departure from Gaussian in the tails on at least one side (for details see Table S1 and Figure S1 in Text S1 of the auxiliary material).[1] This fraction was similar in summer and winter. Three quarters of the stations had at least one variable qualifying as non-Gaussian in each of JJA and DJF. Only 7% of the stations had tails that were consistent with Gaussian within the sampling error bars for all three temperature variables in both seasons.

[18] Asymmetric distributions are very common among those that depart significantly from Gaussian, with the vast majority having a long tail only on one side (high side or low side depending on location). Similar asymmetry in observed tracers and possible causes have been discussed by *Neelin et al.* [2010]. Overall, these tails appear qualitatively consistent with tracer advection prototypes, but the differences in behavior between minimum, maximum and daily averaged temperature and the differences in distribution among different regions suggest the step from qualitative understanding to quantitative simulation may be significant. For most locations, clear departures from Gaussian were confined to the tails, with the core adequately fit by a Gaussian (to within error bars from a Monte Carlo sampling of a synthetic time series). For a few locations, more severe non-Gaussianity was encountered with departures occurring even within the core (as may be seen for Chicago $T_{\min}$ in Figure 1b). In a number of cases with strong asymmetry, fits to the core show shorter-than Gaussian tails occurring on one side (as may be seen for some variables in Figure 1, e.g., for Long Beach, Seattle, Chicago; see also auxiliary material). These are not highlighted here because we do not have as clear a prototype from tracer-advection problems for this behavior at this time. However, this behavior and the physical mechanism for it is important to substantiate in future work. Shorter-than-Gaussian tails would have the converse consequences for change of threshold exceedances under global warming than the long-tailed case discussed below, in some cases enhancing risk of strong changes in threshold exceedances.

[19] The tail characteristics of regional distributions have a number of potential consequences for threshold exceedances under global warming. While only the simplest case is examined here—that of a large-scale temperature increase causing a shift in mean of the observed distribution—the consequences of tail characteristics are substantial. Locations with high-side tails that are roughly Gaussian, such as Phoenix and Houston, have a much higher increase of exceedances of a high threshold value for a given warming shift than do those with prominent high-side exponential tails, such as coastal Los Angeles. In other words, under a given warming a Gaussian-tailed region tends to be at greater risk of heat wave events that have seldom been encountered than a comparable long-tailed region. In the latter, an increase in heat waves exceeding a given threshold does occur but the region is more likely to have experienced such extremes in the past and thus to have infrastructure which is adapted to such occurrences.

[20] The sensitive dependence of tail characteristics on regional effects noted here suggests that it will be (i) useful to understand the physical mechanisms that produce them (including the observed asymmetry, and the sources of regional dependence); and (ii) essential to verify whether high-resolution models accurately reproduce observed tail characteristics for any region for which an assessment of extreme events is being conducted. A model that has an error in the nature of the tail, e.g., erroneously produces a Gaussian rather than a long tail under current climate for a particular region, will likely have serious errors in quantitatively predicting the increase in exceedances under future climate.

[21] **Acknowledgments.** This work was supported in part by National Science Foundation grant AGS-1102838 and National Oceanic and Atmospheric Administration grants NA08OAR4310597 and MAPP10689676. The authors thank J.E. Meyerson for assistance with data and graphics.

[22] The Editor thanks the anonymous reviewer for their assistance in evaluating this paper.

[1] Auxiliary materials are available in the HTML. doi:10.1029/2011GL050610.

References

Alexander, L. V., et al. (2006), Global observed changes in daily climate extremes of temperature and precipitation, *J. Geophys. Res.*, *111*, D05109, doi:10.1029/2005JD006290.

Bourlioux, A., and A. J. Majda (2002), Elementary models with probability distribution function intermittency for passive scalars with a mean gradient, *Phys. Fluids*, *14*, 881–897.

Caesar, J., L. Alexander, and R. Vose (2006), Large-scale changes in observed daily maximum and minimum temperatures: Creation and analysis of a new gridded data set, *J. Geophys. Res.*, *111*, D05101, doi:10.1029/2005JD006280.

Christensen J. H., et al. (2007), Regional climate projections, in *Climate Change 2007: The Physical Science Basis. Contribution of Working Group I to the Fourth Assessment Report of the Intergovernmental Panel on Climate Change*, edited by S. Solomon et al., pp. 847–940, Cambridge Univ. Press, Cambridge, U. K.

Diffenbaugh, N. S., J. S. Pal, R. J. Trapp, and F. Giorgi (2005), Fine-scale processes regulate the response of extreme events to global climate change, *Proc. Natl. Acad. Sci. U. S. A.*, *102*, 15,774–15,778.

Diffenbaugh, N. S., J. S. Pal, F. Giorgi, and X. Gao (2007), Heat stress intensification in the Mediterranean climate change hotspot, *Geophys. Res. Lett.*, *34*, L11706, doi:10.1029/2007GL030000.

Easterling, D. R., J. L. Evans, P. Y. Groisman, T. R. Karl, K. E. Kunkel, and P. Ambenje (2000), Observed variability and trends in extreme climate events: A brief review, *Bull. Am. Meteorol. Soc.*, *81*, 417–425.

Kharin, V. V., and F. W. Zwiers (2005), Estimating extremes in transient climate change simulations, *J. Clim.*, *18*, 1156–1173.

Kharin, V. V., F. W. Zwier, and G. C. H. X. Zhang (2007), Changes in temperature and precipitation extremes in the IPCC ensemble of global coupled model simulations, *J. Clim.*, *20*, 1419–1444.

Lott, N., R. Vose, S. A. Del Greco, T. F. Ross, S. Worley, and J. L. Comeaux (2008), The integrated surface database: Partnerships and progress, paper presented at 88th AMS Annual Meeting, Am. Meteorol. Soc., New Orleans, La., 20–25 Jan.

Majda, A. J., and B. Gershgorin (2010), Quantifying uncertainty in climate change science through empirical information theory, *Proc. Natl. Acad. Sci. U. S. A.*, *107*, 14,958–14,963.

Majda, A. J., and B. Gershgorin (2012), Link between statistical equilibrium fidelity and forecasting skill for complex systems with model error, *Proc. Natl. Acad. Sci. U. S. A.*, in press.

Meehl, G. A., et al. (2007), Global climate projections, in *Climate Change 2007: The Physical Science Basis. Contribution of Working Group I to the Fourth Assessment Report of the Intergovernmental Panel on Climate Change*, edited by S. Solomon et al., pp. 747–845, Cambridge Univ. Press, Cambridge, U. K.

Meehl, G. A., W. D. Collins, B. A. Boville, J. T. Kiehl, T. M. L. Wigley, and J. M. Arblaster (2000), Response of the NCAR climate system model to increased CO_2 and the role of physical processes, *J. Clim.*, *13*, 1879–1898.
Neelin, J. D., B. R. Lintner, B. Tian, Q. Li, L. Zhang, P. K. Patra, M. T. Chahine, and S. N. Stechmann (2010), Long tails in deep columns of natural and anthropogenic tropospheric tracers, *Geophys. Res. Lett.*, *37*, L05804, doi:10.1029/2009GL041726.
Ngan, K., and R. T. Pierrehumbert (2000), Spatially correlated and inhomogeneous random advection, *Phys. Fluids*, *12*, 822–834.
Parmesan, C., T. L. Root, and M. R. Willig (2000), Impacts of extreme weather and climate on terrestrial biota, *Bull. Am. Meteorol. Soc.*, *81*, 443–450.
Peterson, T., and R. Vose (1997), An overview of the global historical climatology network temperature database, *Bull. Am. Meteorol. Soc.*, *78*, 2837–2849.
Pierrehumbert, R. T. (2000), Lattice models of advection-diffusion, *Chaos*, *10*, 61–74.
Schlenker, W., and M. J. Roberts (2009), Nonlinear temperature effects indicate severe damages to us crop yields under climate change, *Proc. Natl. Acad. Sci. U. S. A.*, *106*, 15,594–15,598.
Simolo, C., M. Brunetti, M. Maugeri, T. Nanni, and A. Speranza (2010), Understanding climate change–induced variations in daily temperature distributions over Italy, *J. Geophys. Res.*, *115*, D22110, doi:10.1029/2010JD014088.
Sura, P., and M. Perron (2010), Extreme events and the general circulation: Observations and stochastic model dynamics, *J. Atmos. Sci.*, *67*, 2785–2804.
Sura, P., and P. D. Sardeshmukh (2008), A global view of non-Gaussian SST variability, *J. Phys. Oceanogr.*, *38*, 639–647.
Trenberth K. E., et al. (2007), Observations: Surface and atmospheric climate change, in *Climate Change 2007: The Physical Science Basis. Contribution of Working Group I to the Fourth Assessment Report of the Intergovernmental Panel on Climate Change*, edited by S. Solomon et al., pp. 235–336, Cambridge Univ. Press, Cambridge, U. K.
Walker, M., and N. Diffenbaugh (2008), Evaluation of high-resolution simulations of daily-scale temperature and precipitation over the United States, *Clim. Dyn.*, *33*, 1131–1147.
Walsh, J. E., A. S. Phillips, D. H. Portis, and W. L. Chapman (2001), Extreme cold outbreaks in the United States and Europe, *J. Clim.*, *14*, 2642–2658.

J. D. Neelin and T. W. Ruff, Department of Atmospheric and Oceanic Sciences, University of California, 405 Hilgard Ave., Los Angeles, CA 90095-1565, USA. (neelin@atmos.ucla.edu; truff@atmos.ucla.edu)